Journal of Cleaner Production 115 (2016) 337–342

Contents lists available at ScienceDirect

Journal of Cleaner Production

journal homepage: www.elsevier.com/locate/jclepro

Note from the field

Recyclable magnetite-loaded palm shell-waste based activated carbon for the effective removal of methylene blue from aqueous solution

Kien Tiek Wong [a], Nguk Chin Eu [a], Shaliza Ibrahim [a], Hyunook Kim [b], Yeomin Yoon [c], Min Jang [a, d, *]

[a] Department of Civil Engineering, Faculty of Engineering, University of Malaya, Kuala Lumpur 50603, Malaysia
[b] Dept. of Environmental Engineering, The University of Seoul, Seoul 130-743, Republic of Korea
[c] Department of Civil and Environmental Engineering, University of South Carolina, Columbia, SC 29208, USA
[d] Nanotechnology and Catalysis Research Centre (NANOCAT), University of Malaya, Kuala Lumpur 50603, Malaysia

ARTICLE INFO

Article history:
Received 1 July 2015
Received in revised form
9 December 2015
Accepted 17 December 2015
Available online 30 December 2015

Keywords:
Palm shell-waste based activated carbon
Magnetite
Methylene blue
Removal

ABSTRACT

Magnetized palm shell-waste based activated carbon (MPBAC) was prepared using a simple impregnation of magnetite into palm shell-waste based activated carbon (PBAC) and used for the removal of methylene blue (MB) from an aqueous solution. Based on the isotherm results, MPBAC with the smallest particle size had the highest maximum adsorption capacity (Q_{max} = 163.3 mg g^{-1}). Overall, the kinetic rates of MPBACs were slower than pristine PBACs due to the deposition of magnetite mostly on the outer surface. However, MB was electrostatically attracted towards the magnetite existing at the inner-pores and eventually adsorbed on the interface between the magnetite and the hydrophobic pore surface leading to high sorption density. The thermal regeneration indicated the removal capacities of MB by MPBAC were steady and higher than PBAC for repeated sorption. Through interpretation of thermogravimetric analysis and differential scanning calorimetry, the desorption energy of MB was lowered by the magnetite, leading to better regeneration ability for MPBAC.

1. Introduction

Methylene blue (MB), a cationic dye, is the most often used dye in its category, is known to cause problems in aquatic environments and on human health (Senthilkumaar et al., 2005; Tan et al., 2008). To remediate dye contaminated wastewater, physical and chemical methods such as coagulation-flocculation, precipitation, and oxidation have been thoroughly researched. However, these methods have inherent constraints due to their high cost, high energy requirements, and generation of hazardous by-products (Padmesh et al., 2006; Srivastava et al., 2007). To adopt a zero waste policy, many research studies have been conducted by utilizing carbonaceous waste, especially from the agriculture sector to prepare activated carbon (AC) (Kang et al., 2013; Ozbay and Yargic, 2015; Sayğılı et al., 2015). AC is superior in many aspects, but difficulties encountered during separating spent AC and poor regeneration limit its potential usage in the treatment system. Acid-base regeneration (Qimeng et al., 2015) shows a remarkable regeneration capability, but, the acidic condition could destabilize the coated magnetite. In this research, we used a cheap and widely available material, palm shell-waste based AC (PBAC), as a potential adsorbent for magnetic modification. The main objectives were to develop an economical sorption material which is magnetically separable and recycled at low temperatures. Optimization was conducted by loading magnetite onto different sizes of PBAC to compare the sorption rate and capacity.

2. Experimental

2.1. Materials

PBACs with different mesh sizes (20 × 40, 40 × 60, and 100 × 200) were purchased from Bravo Green Sdn Bhd, Kuching, Malaysia. MB, iron (II) sulfate heptahydrate ($FeSO_4 \cdot 7H_2O$), and sodium hydroxide (NaOH) were purchased from R&M Chemical.

* Corresponding author. Department of Civil Engineering, Faculty of Engineering, University of Malaya, Kuala Lumpur 50603, Malaysia. Tel.: +60 3 7967 7649.
E-mail addresses: minjang@um.edu.my, heejaejang@gmail.com (M. Jang).

http://dx.doi.org/10.1016/j.jclepro.2015.12.063
0959-6526/

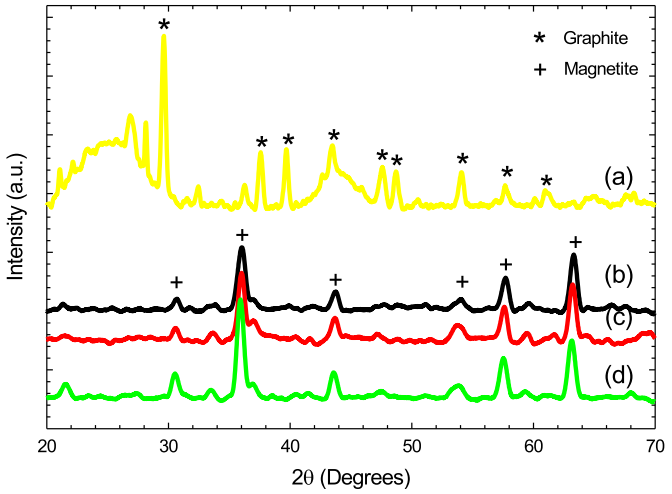

Fig. 1. XRD patterns of (a) PBAC, (b) 100 × 200 MPBAC, (c) 40 × 60 MPBAC, (d) 20 × 40 MPBAC.

2.2. Preparation of magnetized palm shell-waste based activated carbon (MPBAC)

First, 2.8 g of $FeSO_4 \cdot 7H_2O$ were dissolved in 100 mL of distilled water. Then, 0.5 g of PBAC was added to the solution, and the suspension was stirred continuously. While stirring, 10 mL of 1 M NaOH were added drop-wise for 5 min, to precipitate iron (II) hydroxide from the aqueous solution. Subsequently, the solution was heated in a sonicator at 80 °C for 1 h. After cooling, the resulting magnetic adsorbent was washed with distilled water repeatedly until a neutral pH was achieved. Finally, the magnetized palm shell-waste based activated carbon (MPBAC) was dried in an incubator at 80 °C. A similar method was applied to all sizes of PBAC; these are denoted as MPBAC (mesh size). Characterization of adsorbents, sorption isotherms/kinetics, and thermal regeneration were described in Supporting Information (SI).

3. Results and discussion

3.1. Texture and surface characterization of MPBAC adsorbent

Fig. 1 shows the X-ray powder diffraction (XRD) analysis of PBAC and MPBACs. For the pattern of PBAC, the primary diffraction peaks at 2θ of 30°, 37°, and 40° correspond to crystalline graphite, and the other smaller and broader peaks (21°, 48°, 49°, 54°) indicate amorphous carbon. In the XRD patterns of MPBACs shown in curves (b), (c), and (d), the peaks at 2θ of 29°, 35°, 43°, 54°, 57°, and 63° match the standard peaks of magnetite (JCPDS No. 96-900-2321). Furthermore, the graphite peaks disappeared in MPBAC due to the whole coverage of the outer surface by magnetite.

Morphologies of PBAC and MPBAC 100 × 200 were investigated by field emission scanning electron microscopy (FESEM) (Fig. 2), and energy dispersive spectroscopy (EDS) analysis confirmed the presence of Fe. The magnetite was dispersed uniformly on the surface of MPBAC in nanoscale (<200 nm).

The N_2 adsorption–desorption isotherms at 77 K of PBAC and MPBACs are shown in Fig. 3 (a–c). The adsorption isotherms of the PBAC resemble type I isotherms, as defined by IUPAC, indicating the presence of large fractions of micropores, due to the high adsorption at a low relative pressure. The marked knee located in the low relative pressure region, and the very low slope in the multilayer indicate a low external surface and insignificant mesoporosity. With the impregnation of magnetite, the graph shows type IV isotherm at a high relative pressure (P/P_0 = 0.9–1.0), indicating formation of macropores between the magnetite nanoparticles. The pore size distribution graphs presented in Fig. 3(d–f) indicate a reduction in mesopore volume with a slight increase in macropore volume because of magnetite impregnation.

Brunauer, Emmett and Teller (BET) surface area (731.5 $m^2\ g^{-1}$) and total pore volume (0.38 $cm^3\ g^{-1}$) of PBAC 100 × 200

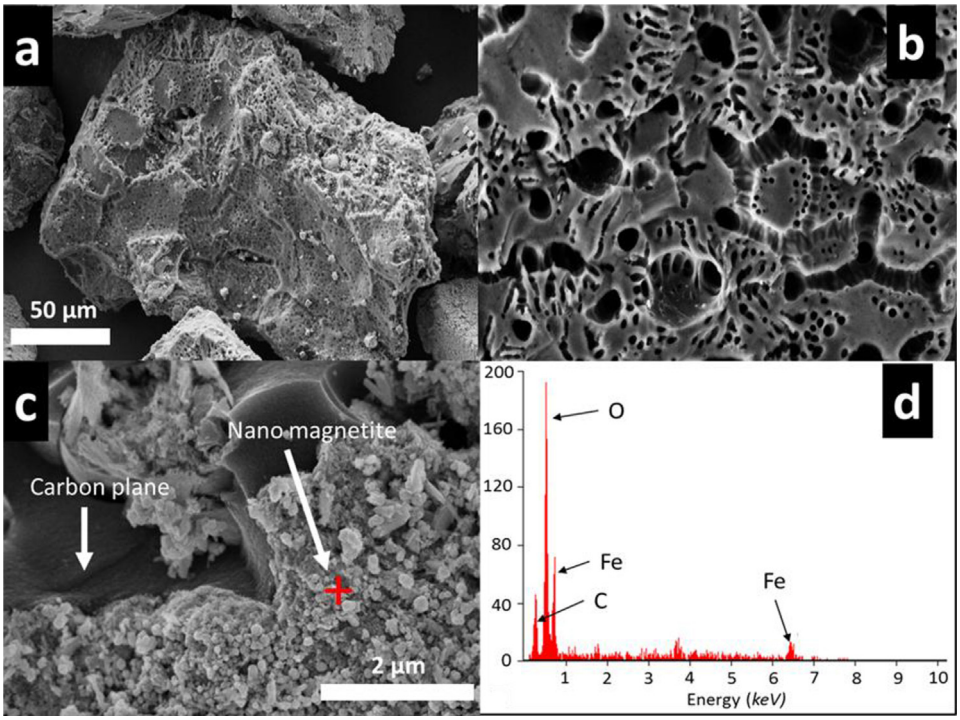

Fig. 2. (a, b) FESEM images of PBAC 100 × 200, (c) MPBAC 100 × 200 and (d) EDX spectrum collected from MPBAC 100 × 200.

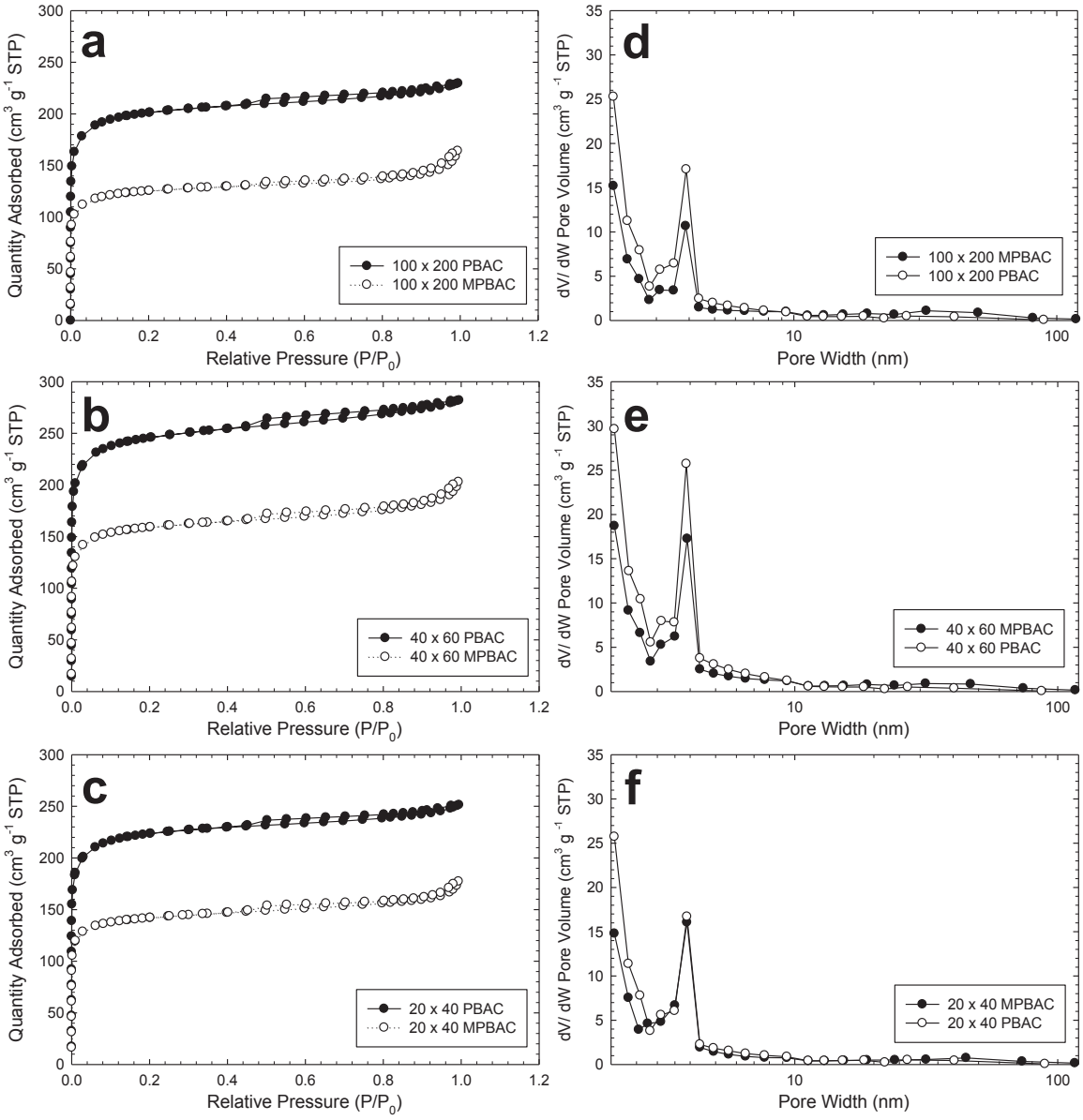

Fig. 3. (a–c) Nitrogen adsorption isotherms at 77 K on different sized PBACs and MPBACs, (d–f) pore size distribution of PBACs and MPBACs.

decreased as magnetite was impregnated onto the MPBACs. The MPBAC 100 × 200 shows the highest reduction in BET surface area (42%), total pore volume (34.2%), and micropore volume (43.5%).

The iron contents in the MPBACs were determined with the aqua-regia method. The Fe concentrations were found to be 483.1, 466.3, and 363.5 mg g^{-1} in MPBAC 20 × 40, 40 × 60, and 100 × 200, respectively. The amount of iron extracted from MPBAC 100 × 200 was the lowest because the Fe ions diffused deep into the micropores, and the aqua-regia method cannot extract total Fe in micropores. This corresponds to the results of the reduction in pore volume and surface area.

The saturation magnetization (M_s) values for MPBACs with different mesh sizes of 20 × 40, 40 × 60, and 100 × 200 were 2.31, 3.53, and 0.57 emu g^{-1} (emu – electromagnetic unit), respectively. The degree of M_s may be linked to the amount of magnetite, although the phase and location of magnetite also affect M_s.

3.2. Adsorption kinetics

Adsorption kinetics define the MB uptake rate and express the efficiency of the adsorption process and the behavior of the adsorbent. In this study, three kinetic models were adopted: pseudo first-order, pseudo second-order, and intraparticle diffusion (IPD; see SI). Fig. 4(a–c) shows the kinetic data of MB removal by different sized PBACs and MPBACs, as well as fit lines using the pseudo second-order kinetic model. Based on R^2 values, kinetic data for PBAC 40 × 60 and 100 × 200 had a better fit to a pseudo second-order kinetic model, while the pseudo first-order best fit the other adsorbents. The high removal rate at the initial 100 min was due to the availability of active sites. As MB fill the vacant pores over time, the number of free binding sites decreases, resulting in a slower rate; this subsequently leads to a plateau condition. The highest initial sorption (v_o), in descending order, were PBAC 100 × 200, PBAC 40 × 60, 100 × 200, and MPBAC 20 × 40 PBAC.

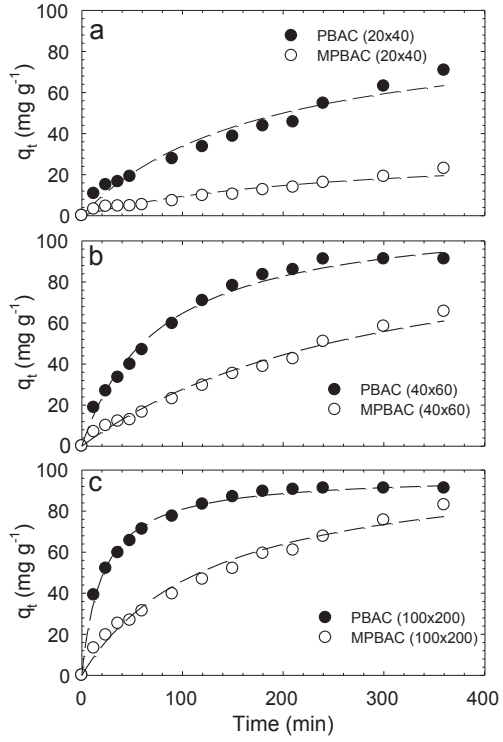

Fig. 4. Adsorption kinetics of MB by various adsorbents (the line curves represent the fit of pseudo second-order kinetic model).

Thus, the particle size of the adsorbents played a dominant role in the amount and rate of MB uptake as smaller particles have a larger external surface area (Wu et al., 2001). Besides, smaller particles exhibited a shorter diffusion pathway into the inner pores. Overall,

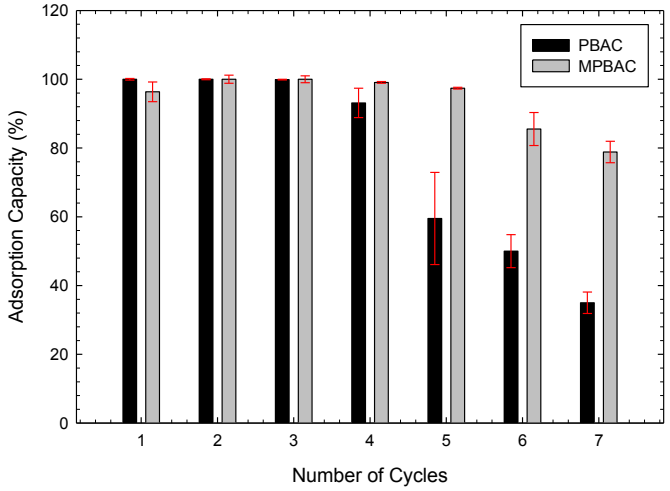

Fig. 6. Adsorption capacities of MB by PBAC/MPBAC (100 × 200) in repeated cycles: 0.02 g media was added into 100 mL of 20 mg L^{-1} MB and operated for 24 h. The media was regenerated for 7 cycles at 350 °C for 3 h.

deposition of magnetite on the outer and inner-pore surface affected the kinetic rate of magnetized AC.

3.3. Adsorption isotherms

In this study, the Langmuir and Freundlich models were used to stimulate the adsorption isotherms. The isotherm parameters that were obtained from both the models and the fittings of these models to the experimental data of MB adsorption are shown in Fig. 5. The equilibrium adsorptions of MB onto MPBACs were fitted by the Freundlich model, indicating that MPBACs have

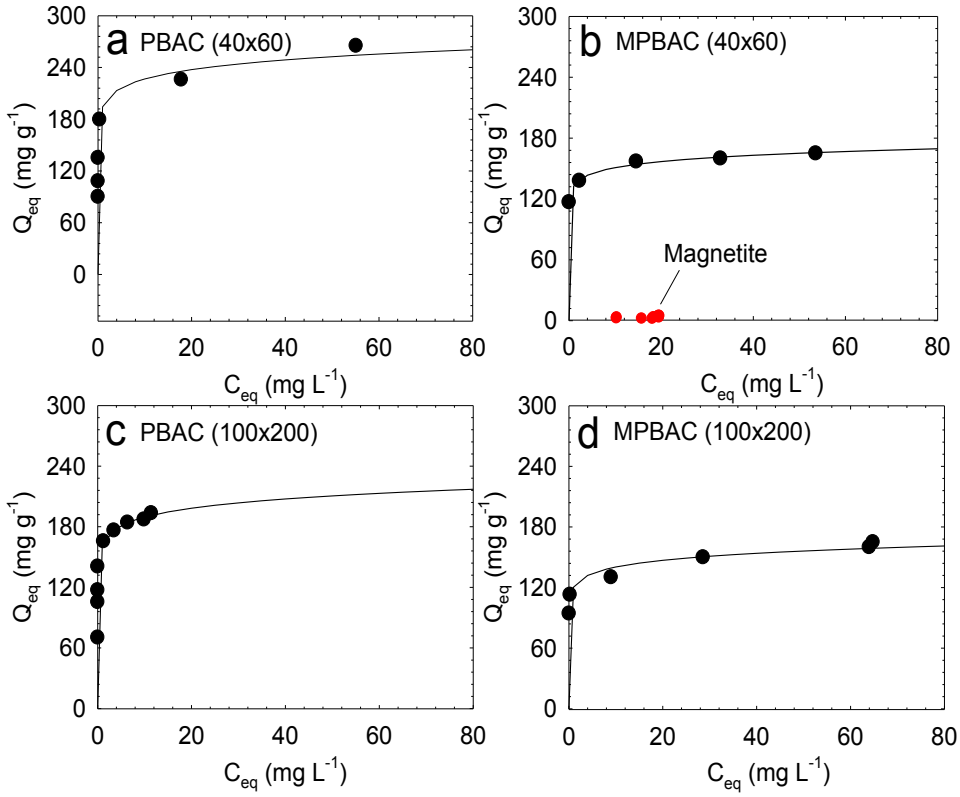

Fig. 5. Adsorption isotherms of MB onto various adsorbents (fit-lines represent Freundlich model).

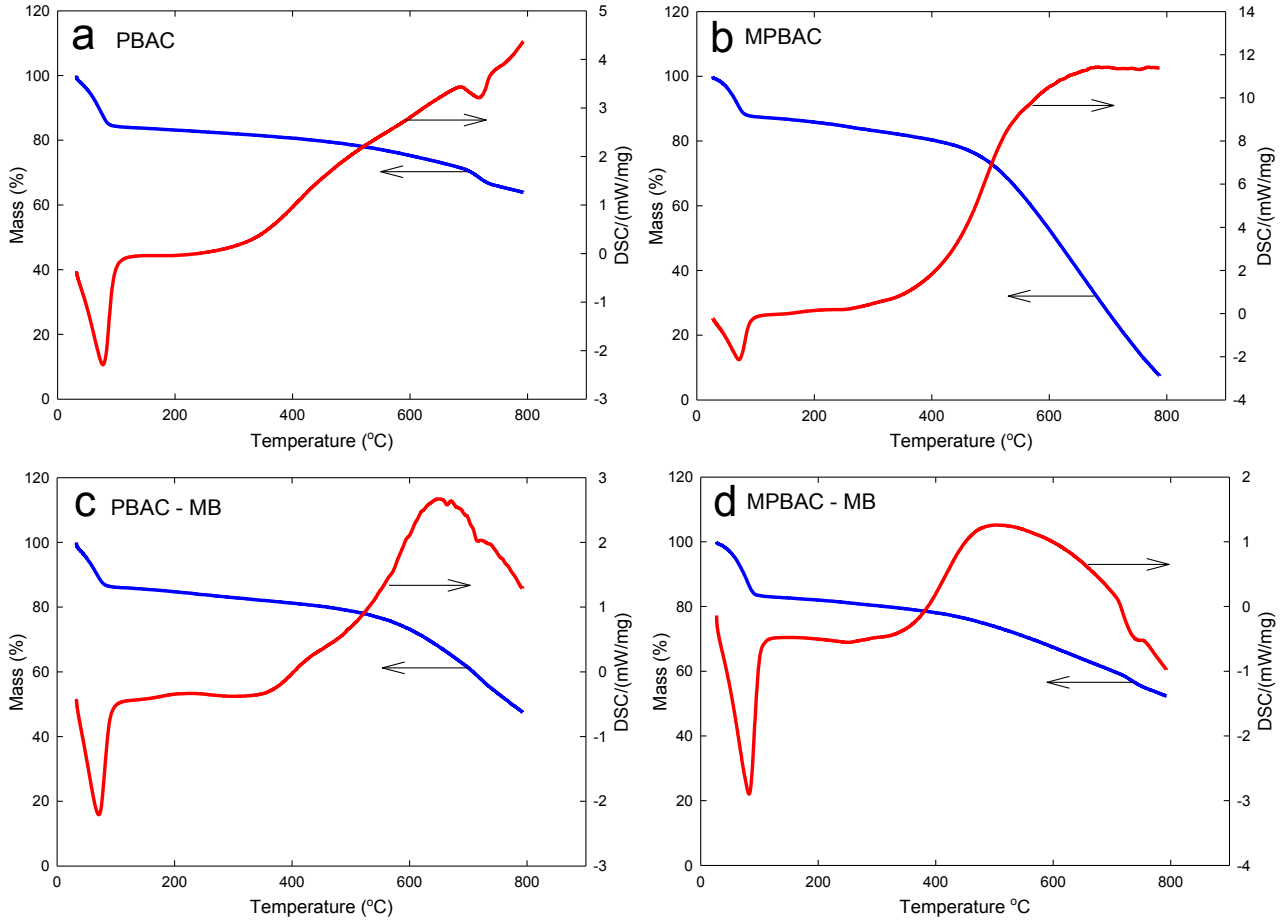

Fig. 7. Thermogravimetric analysis and differential scanning calorimetry results for PBAC and MPBAC (100 × 200) as well as MB saturated media.

heterogeneous sorption sites for MB. As a function of adsorption strength, the value of *1/n* for MPBAC 100 × 200 was 0.056, which is < 1, indicates that the marginal sorption energy decreases with increasing surface concentration (Wu et al., 2009).

Based on the fit of the Langmuir isotherms, PBAC 100 × 200 had the highest maximum adsorption capacity (Q_{max}), followed by PBAC 40 × 60, MPBAC 100 × 200, and MPBAC 40 × 60. This trend is the same as with the kinetic results. By considering sorption density based on micropore surface area, 100 × 200 and MPBACs 40 × 60 showed higher sorption densities of 0.5 and 0.34 mg m^{-2} than PBACs 100 × 200 and 40 × 60, respectively. Thus, compared with pristine PBACs, the magnetite loaded adsorbents showed higher sorption densities. MPBAC 100 × 200 also showed higher sorption capacities than other adsorbents from other references, as shown in SI.

Magnetite was synthesized with the similar method as with MPBAC, and was used for the MB adsorption isotherm. As shown in Fig. 5(b), magnetite itself could not adsorb MB due to the hydrophilic properties of magnetite. Magnetite has a relatively low point of zero charge (pH_{pzc} < 7) (Ai et al., 2011), therefore, the surface of magnetite becomes negatively charged (i.e., Fe—O^-) at a neutral pH. Thus, the kinetic and isotherm results suggest that the magnetite only assists the MB to diffuse into pores through electrostatic interactions, resulting in a higher MB sorption density within the pores. However, the loss of external carbon surface due to magnetite coating caused a decrease in the initial sorption rate. As an ideally planar molecule, MB can be readily adsorbed through π-π electron donor acceptor interactions between the aromatic backbone of MB and the graphene plane of activated carbon (Ai et al., 2011; Yanhui et al., 2013).

3.4. Regeneration

Thermal regeneration at low temperatures has a higher efficiency in regenerating saturated MPBAC 100 × 200 than PBAC 100 × 200 (Fig. 6). The MB adsorption capacities of regenerated MPBAC appeared to recover fully for the first five cycles, but slightly reduced by 16% at the seventh cycle. The adsorption capacities for PBAC 100 × 200 remained constant for the first three cycles, then decreased significantly, by 65%, by the seventh cycle.

Fig. 7 shows the thermal gravimetric analysis (TGA) and differential scanning calorimetry (DSC) results of PBAC, MPBAC, and MB retained adsorbents. MPBAC exhibited a higher mass loss (83%) than PBAC (35%) due to its significant mass loss of magnetite-based oxygen complexes (Bansal et al., 1988; Maroto-Valer et al., 2004). Since magnetite could weaken the thermal stability of the PBAC (Li et al., 2000), it could lead to decomposition of the carbon structure at a lower temperature. PBAC-MB and MPBAC-MB had similar mass losses of ~50%, representing that thermal energy might be used to break the bonding of MB instead of carbon structure. In the DSC profiles, the peak occurred in all the samples at 80–100 °C, indicating an endothermic reaction caused by water vapor present in the pores of the adsorbents (Maroto-Valer et al., 2004). A weak and broad peak at 350 and 250 °C, respectively, can be assigned to the desorption of physi-sorbed MB, while peaks centered at 650 and 500 °C for PBAC-MB and MPBAC-MB, respectively, can be assigned

to the desorption of the chemosorbed fraction. Accordingly, the desorption energy of MB was lowered by coating magnetite onto the PBAC. This is supported by the repeated adsorption results. Based on these results, it can be concluded that magnetite has a catalytic effect on the reduction of desorption energy (Wu et al., 2004; Zhang et al., 2007).

4. Conclusions

An economic carbon material, PBAC, was magnetized via simple impregnation of magnetite and tested for MB removal. Based on the isotherm results of magnetized adsorbents, the smallest MPBAC 100 × 200 mesh had the highest maximum adsorption capacity (Q_{max} = 163.3 mg g^{-1}). Overall, the adsorption rates of MPBACs were slower than pristine PBACs, however, the MB adsorption densities were higher due to electrostatic attraction of negatively charged magnetite. The main adsorption mechanism is π–π electron donor acceptor interactions. MPBAC was found to have better thermal regeneration than PBAC due to magnetite's catalytic effect which reduces the desorption energy of MB. MPBAC could be a promising adsorbent for dye wastewater treatment because of its magnetic recovery and regeneration capability.

Acknowledgment

This project was funded by the Malaysian Government Ministry of Higher Education through the High Impact Research Grant (D000062-16001).

Appendix A. Supplementary data

Supplementary data related to this article can be found at http://dx.doi.org/10.1016/j.jclepro.2015.12.063.

References

Ai, L.H., Zhang, C.Y., Liao, F., Wang, Y., Li, M., Meng, L.Y., Jiang, J., 2011. Removal of methylene blue from aqueous solution with magnetite loaded multi-wall carbon nanotube: kinetic, isotherm and mechanism analysis. J. Hazard. Mater. 198, 282–290.

Bansal, R.C., Donnet, J.B., Stoeckli, F., 1988. Active Carbon. Marcel Dekker, United States.

Kang, Y.L., Seong Khoon, S.T., Monash, P., Ibrahim, S., Saravanan, P., 2013. Adsorption isotherm, kinetic and thermodynamic studies of activated carbon prepared from *Garcinia mangostana* shell. Asia-Pacific J. Chem. Eng. 8, 811–818.

Li, Z.J., Jaroniec, M.T., Choma, J., 2000. Thermogravimetric and adsorption studies of oxidized active carbons by using different probe molecules. Thermochim. Acta 345, 165–172.

Maroto-Valer, M.M., Dranca, I., Lupascu, T., Nastas, R., 2004. Effect of adsorbate polarity on thermodesorption profiles from oxidized and metal-impregnated activated carbons. Carbon 42, 2655–2659.

Ozbay, N., Yargic, A.S., 2015. Factorial experimental design for Remazol Yellow dye sorption using apple pulp/apple pulp carbon–titanium dioxide co-sorbent. J. Clean. Prod. 100, 333–343.

Padmesh, T.V.N., Vijayaraghavan, K., Sekaran, G., Velan, M., 2006. Biosorption of Acid Blue 15 using fresh water *macroalga Azolla filiculoides*: batch and column studies. Dyes Pigments 71, 77–82.

Qimeng, L., Yanshan, Q., Canzhu, G., 2015. Chemical regeneration of spent powdered activated carbon used in decolorization of sodium salicylate for the pharmaceutical industry. J. Clean. Prod. 86, 424–431.

Sayğılı, H., Güzel, F., Önal, Y., 2015. Conversion of grape industrial processing waste to activated carbon sorbent and its performance in cationic and anionic dyes adsorption. J. Clean. Prod. 93, 84–93.

Senthilkumaar, S., Varadarajan, P.R., Porkodi, K., Subbhuraam, C.V., 2005. Adsorption of methylene blue onto jute fiber carbon: kinetics and equilibrium studies. J. Colloid Interf. Sci. 284, 78–82.

Srivastava, V.C., Mall, I.D., Mishra, I.M., 2007. Adsorption thermodynamics and isosteric heat of adsorption of toxic metal ions onto bagasse fly ash (BFA) and rice husk ash (RHA). Chem. Eng. J. 132, 267–278.

Tan, I.A.W., Ahmad, A.L., Hameed, B.H., 2008. Adsorption of basic dye using activated carbon prepared from oil palm shell: batch and fixed bed studies. Desalination 225, 13–28.

Wu, F.-C., Tseng, R.-L., Juang, R.-S., 2001. Adsorption of dyes and phenols from water on the activated carbons prepared from corncob wastes. Environ. Technol. 22, 205–213.

Wu, F.-C., Tseng, R.-L., Juang, R.-S., 2009. Initial behavior of intraparticle diffusion model used in the description of adsorption kinetics. Chem. Eng. J. 153, 1–8.

Wu, R.C., Qu, J.H., He, H., Yu, Y.B., 2004. Removal of azo-dye Acid Red B (ARB) by adsorption and catalytic combustion using magnetic $CuFe_2O_4$ powder. Appl. Catal. B Environ. 48, 49–56.

Yanhui, L., Qiuju, D., Tonghao, L., Xianjia, P., Junjie, W., Jiankun, S., Yonghao, W., Shaoling, W., Zonghua, W., Yanzhi, X., 2013. Comparative study of methylene blue dye adsorption onto activated carbon, graphene oxide, and carbon nanotubes. Chem. Eng. Res. Des. 91, 361–368.

Zhang, G., Qu, J., Liu, H., Cooper, A.T., Wu, R., 2007. $CuFe_2O_4$/activated carbon composite: a novel magnetic adsorbent for the removal of acid orange II and catalytic regeneration. Chemosphere 68, 1058–1066.